

Anisotropy of the optical poling of glass

M. K. Balakirev,¹ I. V. Kityk,^{2,3,*} V. A. Smirnov,¹ L. I. Vostrikova,¹ and J. Ebothe⁴

¹*Institute of Semiconductor Physics SB RAS, Acad. Lavrentyev, 13, Novosibirsk 630090, Russia*

²*Institute of Physics WSP, PL-42217, ulnica Gombrowicza 1/144, Częstochowa, Poland*

³*Institute of Computer Modelling, Krakow University of Technology, ulnicka Warsawian 24, Krakow, Poland*

⁴*Université de Reims, UTAP-LMET, EA No. 2061, UFR Sciences, Boîte Postale 138, 21 Rue Clement Ader, Reims, France*

(Received 13 August 2002; published 13 February 2003)

A giant reversible increase ($\geq 10^3$ times) of the optical second-order harmonic's (SH) absorption by optical poling of oxide glass was found. The SH's absorption kinetics manifested anisotropy with respect to polarization of the pumping (poling) light. The observed absorption exerts the influence of optical poling on the observed processes and leads to a limitation of the maximum value of the photoinduced SH output in oxide glass. An explanation of the observed phenomenon is given. It was shown that the observed process is a typical steady-state effect with participation of trapping levels, and its polarized dependence is caused by the photoinduced anisotropy of the photocarrier diffusion and by the electron-phonon anharmonic interaction.

DOI: 10.1103/PhysRevA.67.023806

PACS number(s): 42.65.Hw, 78.20.Ci

I. INTRODUCTION

The optical poling of oxide glasses was first observed in the Ref. [1]. In Ref. [2] a little absorption (up to 2%) of the total second-order harmonic (SH) signal was found. However, among the large number of references devoted to optical poling [3–14], the problem of anisotropy in absorption kinetics during the optical treatment has not yet been investigated. This effect may have an important application aspect, particularly during design of nonlinear optical filters, for the achievement of desired phase-matching conditions, etc. Simultaneously, such kinds of experiments could give additional information for clarification of the cascading steady-state processes during optical poling.

In the present work we present experimental investigations of the photoinduced SH kinetics, particularly its anisotropy for different polarizations of the induced light in the oxide glass. We will try to separate optical poling (steady-state process) from other effects (e.g., photodarkening and bleaching, self-focusing, higher-harmonic generation, etc.) and to give an explanation of the phenomenon within a framework of the existing phenomenological and microscopic models.

It is well known that illumination of glasses by two mutually coherent beams with fundamental and doubled frequencies leads to the formation of a long-lived reversible electrostatic polarization [3–8]. This process is known as optical poling [3]. During optical poling, glass changes its symmetry and acquires the properties of a single-axis crystal. Therefore the second-harmonic generation (SHG) [3,5–13] and the parametric amplification [14] described by polar third-rank tensors may be allowed by symmetry in such media.

In the case of oxide glasses, the optical poling is caused [5] by the formation of a spatially periodic optically induced electrostatic field $\mathbf{E}_0(\mathbf{r})$ in the sample due to photocarrier charge separation by means of direct current due to a coher-

ent photogalvanic effect [15,16]. The latter corresponds to the coherent nonlinear photon interaction $\omega + \omega - 2\omega \rightarrow 0$ favoring the creation of a nonzero coherent photocurrent:

$$\mathbf{J} = \mathbf{e}_j A_1^2 A_2 \cos(\mathbf{q} \cdot \mathbf{r}). \quad (1)$$

A basic peculiarity of this poling is a spatial periodicity of the photoinduced field with a period of q^{-1} ($\mathbf{q} = 2\mathbf{k}_1 - \mathbf{k}_2$, \mathbf{k}_1 and \mathbf{k}_2 are wave vectors of fundamental and doubled-frequency coherent beams). Therefore, the periodic space modulation of the refractive index $\Delta n_{ij} \sim \chi_{ijkl}^{(3)} E_{0k} E_{0l}$ with a period of $(2q)^{-1}$ (anisotropic Δn_{ij} grating [4]) and the second-order effective polarizability $\chi_{ijk}^{(2)} \sim \chi_{ijkl}^{(3)} E_{0l}$ with the period of q^{-1} ($\chi_{ijk}^{(2)}$ grating [5]) appears due to the optical poling of oxide glass. By certain angles of the convergent beams, the creation of the grating leads to a self-diffraction of the incident light [3]. The spatial periodicity of $\chi_{ijk}^{(2)}$ favors an effective SHG [5–14] and the parametric amplification of light [14], since the process of light conversion in this grating is phase matched.

The photoinduced SH was investigated by optical poling of different oxide bulk glasses and fibers [3–6]. However, its efficiency ($\sim 5\%$), which was observed [6] in a germanosilicate glass, was the maximal obtained to date. So the main problem consists in the clarification of the origin of the observed limitation of the optical poling.

In the present paper we study the giant enhancement ($\geq 10^3$ times) of the SH's absorption by the optical poling of oxide glass. Particular attention is devoted to the anisotropy of absorption kinetics during optical poling and to the clarification of the origin of the cascading steady-state processes in the observed phenomenon with the participation of trapping levels and electron-phonon interaction.

II. MEASUREMENT TECHNIQUE

The experiments were conducted in the prefabricated measuring glass plate PM40 (oxide glass Russian trademark K8). The glasses with this sort of trademark are used for the production of different optical elements such as the plates,

*Email address: i.kityk@wsp.czest.pl

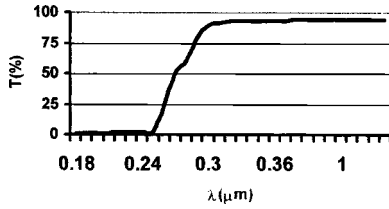


FIG. 1. Transparency of the investigated glasses (sample's thickness of about 4 cm).

lenses, prisms, etc. The chemical analysis of the glass gives the following content: SiO_2 (51.7 wt. %), BaO (24.8 wt. %), K_2O (5.3 wt. %), Na_2O (2.1 wt. %), Fe_2O_3 (0.16 wt. %). The refractive indices and absorption coefficients for wavelength $\lambda_1 = 1.079 \mu\text{m}$ are $n_1 = 1.506$, $\alpha_1 = 0.003 \text{ cm}^{-1}$ and those for wavelength $\lambda_2 \approx 0.54 \mu\text{m}$ are $n_2 = 1.518$, $\alpha_2 = 0.003 \text{ cm}^{-1}$, respectively [17]. Their transparent spectra are presented in the Fig. 1. The photoinduced SH in the glass with this trademark was first observed in the Ref. [1]. The experimental setup is presented in the Fig. 2.

The fundamental frequency radiation of pulsed Nd:YAlO₃ laser (with $\lambda_1 = 1.079 \mu\text{m}$, duration of the laser pulses ≈ 15 ns, pulse energy ≈ 16 mJ, repetition frequency 12.5 Hz) was converted into the radiation of doubled frequency ($\lambda_2 \approx 0.54 \mu\text{m}$) in a CDA crystal possessing a conversion efficiency about 10%. The set of mirrors and filters was used for the space separation of the beams. The filtering system allowed us to obtain a sufficiently pure monochromatic beam (the attenuation of the intensity of the additional component of radiation in each separated channel was more than 10^{10}). After the separation of the fundamental and doubled beams, they were focused and intersected inside the sample at the angle θ . The beams were polarized in the plane of their convergence. The diameters of the beams at the focal point were about 260 and 170 μm for the fundamental and doubled harmonic frequencies, respectively. The typical laser power densities at the waist were $I_\omega \approx 4 \text{ GW/cm}^2$ and $I_{2\omega} \approx 0.4 \text{ GW/cm}^2$, respectively.

During the illumination of the glass with two frequencies (during the process of optical poling) the optically induced field grating E_0 , and Δn and $\chi^{(2)}$ gratings were localized in the region of the beam interactions. We have chosen the

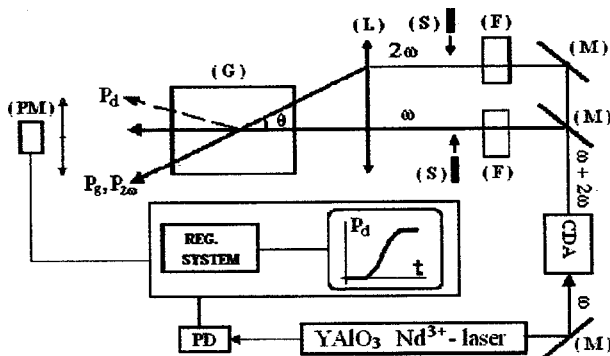


FIG. 2. Experimental setup: *M*, mirrors; *F*, filters; *S*, opaque shades; *PM*, photomultiplier; *L*, spherical lens; *G*, sample (glass); *CDA*, frequency-doubled crystal; *PD*, photodiode.

angle θ between the incident beams in such a way that the grating Δn was oriented at the Bragg angle with respect to the incident beam of the fundamental frequency: $\theta = \arccos[(3\eta^2 + 2)/5\eta]$, where $\eta = n_1/n_2$. In this case the maximum efficiency of the diffraction for the incident light with the fundamental frequency was observed on the induced Δn grating. The diffracted beam emerged from the sample at the angle $\approx 19.8^\circ$ with respect to the incident beam of the fundamental frequency. In the experiment we had the possibility of detecting simultaneously (independently one after another) the beam that was propagated through the sample radiation of the fundamental, doubled frequency and the diffracted beam for the fundamental frequency, since these beams had different directions of propagation.

To clarify the influence of the photodarkening in the observed phenomenon, we have performed independent measurements of the absorption of the He-Se laser (with power 5 mW, wavelength 514 nm, and spot diameter about 220 μm). To focus the green He-Se laser beam into the diameter of the fundamental beam, a special diaphragmed slit was attached to the sample. Thus, parallel direction of propagation for the probe He-Se laser and fundamental laser beams was achieved in the same entrance point of the sample. Independently, the setup was verified for the chalcogenide glasses [20] with the known value of the photodarkening. For better signal-to-noise ratio, a DKDP electro-optics modulator (with frequency of modulation about 150 kHz) was used.

Simultaneously with the light diffraction on the Δn grating, the conversion of the fundamental frequency radiation into the second-harmonic radiation took place also in the glass due to the $\chi^{(2)}$ grating. The photoinduced SH propagated along the direction of the propagation of incident beam with the doubled frequency. Therefore, for the monitoring of the photoinduced SH signal we focus the incident beam of the doubled frequency at the entrance of the sample for short time intervals of 5–10 s separated by 3-min intervals.

In the experiments, we detected a peak power $P_d(\omega)$ of the diffracted light on the Δn -grating light of the fundamental frequency, a peak power $P_{2\omega}$ of the beam that was propagated through the sample radiation of the SH, and a peak power $P_g(2\omega)$ of the photoinduced SH on the $\chi^{(2)}$ SH using a photomultiplier in the remote zone. After the photomultiplier, the output analogous signals were transformed by an analog-digital voltage converter and were processed by a computer. The recorded signals were averaged over 15–20 pulses, which decreased the influence of the radiation or noise instability. We used a separate photodiode for control of the time stability of laser radiation. The sensitivity threshold of the measuring system was about 1 $\mu\text{W/pulse}$.

III. RESULTS AND DISCUSSIONS

The measured results are presented in Figs. 3–5. In Fig. 3 (left part), typical time dependences of the P_d , $P_{2\omega}$, and the intensity $I_{2\omega}$ on the axis (a slit $\sim 40 \mu\text{m}$ was in the center of the registered beam) of the light that propagated through the doubled frequency grating are shown during the optical poling up to saturation ($t \approx 70$ min).

One can see from Fig. 3 that the peak power of the dif-

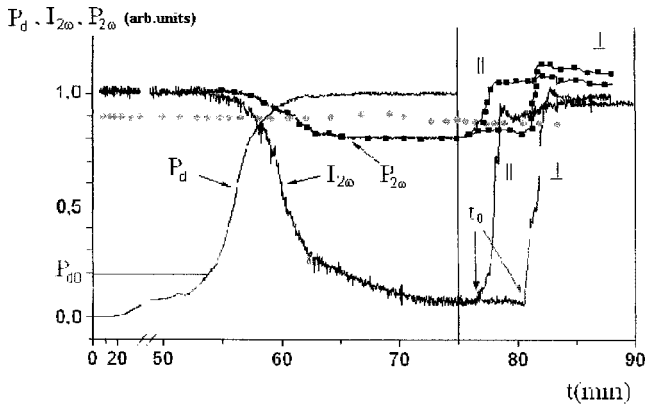


FIG. 3. Time dependence of P_d , $I_{2\omega}$, $P_{2\omega}$ during the optical poling of glass (left part). By the squares are indicated additionally measured power dependencies as described in the text. Evolution of the intensity of the light passing through the grating doubled-frequency radiation with parallel and perpendicular poling light polarization (right part, the basic beam was overlapped at the moment t_0). The dotted points represent the spectral dependence of absorption (in arbitrary units) for the green light measured by spectrophotometric method.

fracted light P_d increases with time and achieves the same steady-state level. It is obvious that the increase of the value P_d is related with an enhancement of the amplitude of the Δn grating with time (with the increasing amplitude of the electric-field grating). Therefore, we have the possibility to monitor the amplitude of the optically induced optical grating by the peak power $P_d(\omega)$ of the diffracted light for the fundamental frequency.

Our experiments show that at some value of the amplitude of the field grating, a strong increase of the light absorption with doubled frequency is observed. As the amplitude of the field grating reaches the value corresponding to the value of the peak power of the diffracted light $P_d = P_{d0}$ (see Fig. 3), the peak power $P_{2\omega}$ passing through the sample radiation of doubled harmonic decreases with time. $P_{2\omega}$ reaches its steady-state level at the same time the P_d (and, correspondingly, the amplitude of the optically induced field grating) reaches its maximum value. The steady-state value of $P_{2\omega}$ is almost 20% less than the initial value of $P_{2\omega}$ (before the beginning of the optical poling process). Thus, the observed integral absorption of the light with doubled frequency is not so large, and adds up to 20% of the total absorption. Some increase of the integral absorption of green light (about 2%) was observed earlier in an optical fiber with the prolonged

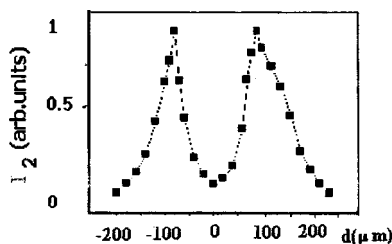


FIG. 4. Radial space profile sequence of the beam's intensity with doubled frequency.

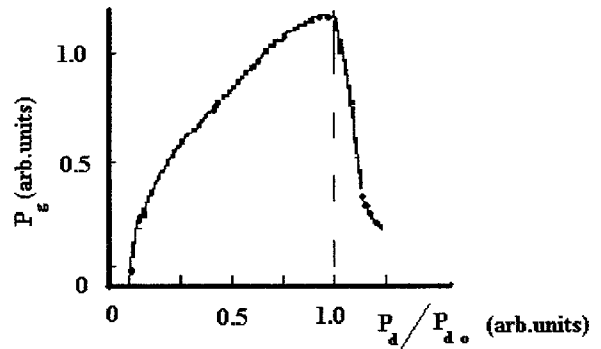


FIG. 5. Dependence of the peak power $P_g(2\omega)$ of the photoinduced SH on the $\chi^{(2)}$ grating on the value of the peak power $P_d(\omega)$ of the self-diffracted light on the Δn -grating light for the fundamental frequency.

passage of mutually coherent bichromatic light with frequencies ω and 2ω through it [18]. Figure 3 clearly demonstrates that the measurement of the absorption for green light (indicated by the dotted line) does not show substantial changes; thus the role of the photodarkening is not so crucial. Absorption caused by electron-phonon trapping levels gives a contribution that is below the spectral range of about 460 nm. So the green light absorption is vanishingly small.

In the steady-state regime we investigated a sequence of the beam profile distribution of the beam that passed through the sample for the doubled frequency. The beam profile sequence was obtained by moving the beam's slit (with width $\approx 20 \mu\text{m}$) in the plane of the convergence of incident beams perpendicular to the direction of propagation of the radiation with doubled frequency. The slit was disposed directly at the entrance to the photomultiplier at a distance of about 2 cm from the backside of the glass, with the step of the scanning being about $20 \mu\text{m}$.

In Fig. 4 are shown the output signals from the photomultiplier that were detected in the presence of the slit at different points of the beam passing through the sample radiation with doubled frequency. The obtained curve displays the distribution of the intensity $I_{2\omega}(d)$ (d is the distance from the center of the beam axis) at the distinct points of the profile sequence of the beam passing perpendicularly to the plane of convergence of the incident beams.

One can see from Fig. 4 a large minimum of $I_{2\omega}$. The absorption of light takes place only in the region in which the induced grating field exists. Since the convergence angle of interacting beams is small, in our experiment the induced electric-field grating has a sufficiently long size ($L \approx 5 \text{ mm}$) along the direction of the propagation of the radiation with a doubled frequency beam, but it has a typical narrow sequence size perpendicular to the direction of the beam propagation. The cross-section size of the optically induced grating is formed by the convolution of the cross distributions of the incident radiation with the fundamental and doubled frequencies and, therefore, is a bit less than the diameter of the incident beam of doubled frequency. As a consequence, the space distribution of the intensity $I_{2\omega}(d)$ of the passed radiation with doubled frequency observed in Fig. 4 includes the picture of the space distribution of the light absorption in the

cross-section plane of the grating. One can see that the maximum absorption is observed on the axis of the doubled-frequency beam where the amplitude of the optical grating has its maximum value. But the absorption decreases strongly in the region of the boundary of the cross section of the field grating. As a result, we observe the integral absorption of light with doubled frequency that is substantially less than the space localized absorption on the beam axis.

Generally, intensity redistribution may be caused by different factors, and absorption in the center of the beam may be one of the possible explanations. For example, such intensity distribution is typical for the behavior of the self-focusing. So one can expect this intensity change due to inertial change in the real part of susceptibility (and related refractive index) due to the poling process. The quantum chemical estimations performed by a method similar to that described in Refs. [19,20] have shown that the contribution due to the nonlinear refractive index n_2 should not exceed 8.7%. So it is not sufficient to cause the observed giant changes presented in Fig. 4.

Another process that could give the contribution to the observed behavior is the fourth-harmonic generation described by the fifth-order optical susceptibility tensors. Using evaluations similar to those for n_2 , we have found that this contribution will give not more than 2% to the observed dependences. A more quantitative analysis of these as well as several other factors will be the subject of a future separate work. However, even from the performed evaluations, one can state that the mentioned contributions are not sufficient for the explanation of the observed phenomenon.

We placed the slit in the center of the registered beam that passed through the grating light with doubled frequency and studied the dependence of the intensity $I_{2\omega}$ on the axis of the propagated beam versus time during the optical poling process. The results of this experiment are presented in Fig. 3 (the curve, which marks as $I_{2\omega}$). One can see that the doubled-frequency radiation, as it passes through the grating, can be attenuated on the beam axis by a factor of 30. If it is assumed that the decay along the length L of the field grating is described by the exponential Lambert law $I_{2\omega} = I_{2\omega,0} \exp(-\alpha L)$, then the observed attenuation corresponds to an absorption value of about $\alpha \approx 7 \text{ cm}^{-1}$. Our estimation of the absorption for the doubled-frequency radiation in the clear glass, which was performed by the observation of the light absorption in two clear samples with different lengths $L = 0.5 \text{ cm}$ and $L = 4 \text{ cm}$ using a spectrophotometer, gives the value $\alpha_2 < 10^{-2} \text{ cm}^{-1}$. The known tabular value of the absorption for the doubled-frequency radiation in the glass with this trademark is $\alpha_2 = 3 \times 10^{-3} \text{ cm}^{-1}$ [17]. So the observed maximal change in the absorption of light compared with the unperturbed sample differs by about three orders of magnitude ($\delta\alpha = \alpha/\alpha_2 \approx 2 \times 10^3$).

We made an additional separate experiment to check the polarization dependence of SH's absorption kinetics. After the optical poling of the glass up to saturation ($t \geq 70 \text{ min}$), the beam of the fundamental frequency was focused and we observed the evolution of the intensity $I_{2\omega}$ on the axis of the beam that passed through the grating light with doubled frequency. The results for two different polarizations of the in-

cident radiation of the doubled frequency are shown in Fig. 3 (right part). In the first case the polarization of light coincided with the polarization of the recording beam. In the second case the polarization was perpendicular. One can see from Fig. 3 (right part) that the absorption reaches the maximum value in the initial time moment. Then it smoothly decreases with time and reaches the same value as it had in the untreated sample. Such behavior is a consequence of the erasure of the grating by the doubled-frequency light [14]. During the erasure of the grating, the absorption of the light decreases. Simultaneously, the observed absorption of the propagated radiation through the field grating with doubled frequency does not depend on its initial polarization. So we do not observe the dichroism of the light absorption inside the optically induced electric-field grating.

The appearance of the large absorption of the radiation with doubled frequency by optical poling should also influence the process of the photoinduced SH and the $\chi^{(2)}$ grating in glass. We detected the value of the peak power $P_g(2\omega)$ of the photoinduced $\chi^{(2)}$ grating during the optical poling process. It was found that at the initial stage the value of the SHG increases with the increasing optically poling field (Fig. 5) [we monitored the amplitude of the optically induced electric-field grating by the peak power $P_d(\omega)$ of the self-diffracted light of the fundamental frequency, as was described above]. However, at the higher values of the poled field (when the $P_d > P_{d0}$), the peak power of the SHG decreases with the increasing amplitude of the effective electric field. The beginning of the decrease of the photoinduced SH signal (about the $P_d = P_{d0}$) coincides with the beginning of the observed absorption of light for doubled frequency in our sample (see Figs. 3 and 5). So, it is experimentally confirmed that the observed absorption is caused by the restriction of the maximum value of the photoinduced SH in the glass.

To clarify the behavior of the power's kinetics for the two orthogonal laser beams, we have carried out independent measurements of the laser powers for two orthogonal polarizations using the laser power controller BFOC with the RS-232 interface. From Fig. 3 one can see a sufficiently good (see squared curve) correlation of the observed power dependences with the dependences of the laser intensities, which means that the observed anisotropy is caused mainly by the difference in the absorption edge.

The observed integral absorption of light in the region of the high amplitude of the optically induced electrostatic field gives additionally only several percent contribution, and is substantially less than the local absorption near the beam axis. Therefore, the phenomenon of the giant increase of the local optical SH's absorption, which is observed during the optical poling of the medium in the region of the high amplitudes of the induced field grating, could remain as an undiscovered one in the experiments of other authors in oxide bulk glasses and fibers. However, this phenomenon is crucial for the investigations, since it limits the optical poling technique.

To understand the long-living poling processes we consider the principal features of the band energy structure in oxide glasses. It is well known that all the glasses are characterized by an intermediate structural ordering. At the same time, the considered oxide glasses are typical disordered di-

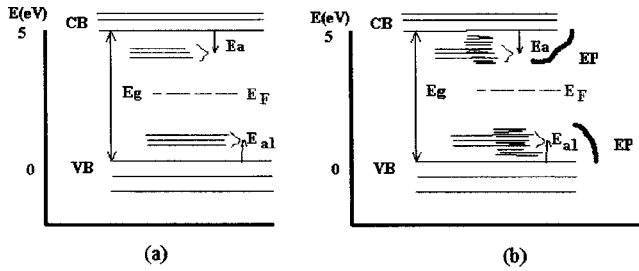


FIG. 6. Principal schema of the energy structure for the nonilluminated glass (a). Principal band structure of the glass taking into account the photoinduced electron-phonon trapping states (b).

electrics with effective energy gaps of about 5 eV. As a consequence, one can expect the occurrence of a large number of trapping states within the energy gap (see Fig. 6). The electron states in the energy gap are localized in space and possess relatively uniform energy spectrum. The low absorption of the glass (Fig. 1) in the visible spectral region additionally confirms this model.

The nonlinear interaction of two coherent electromagnetic waves (fundamental beam and its second harmonics) leads to the appearance of the coherent photocurrent [Eq. (1)] and the superposition of the periodic optically induced electrostatic field \mathbf{E}_0 in accordance with Maxwell's electrodynamics equations:

$$\frac{d\rho}{dt} = \text{div}(\mathbf{J} + \mathbf{J}_c), \quad \text{div}(\varepsilon \mathbf{E}_0) = -4\pi\rho. \quad (2)$$

Here $\mathbf{J}_c = \sigma \mathbf{E}_0$ is the conduction current. A solution of Eq. (2) gives

$$\mathbf{E}_0(\mathbf{r}, t) = \frac{1}{\sigma} \mathbf{A}_0(\mathbf{r}) \cos(\mathbf{q} \cdot \mathbf{r}) [1 - \exp(-4\pi\sigma t/\varepsilon)]. \quad (3)$$

The amplitude $\mathbf{A}_0(\mathbf{r})$ depends on the spatial distribution of the interacting beams.

Moreover, the formation of the optically induced electric field in the medium leads to appearance of the electromagnetically induced SH described by a third-rank polar tensor $\chi_{ijk}^{(2)} = \chi_{ijkl}^{(3)} E_{0l}$ and the optically induced scattering of light on the additional birefringence $\Delta n_{ij} \sim \chi_{ijkl}^{(3)} E_{0k} E_{0l}$ (analogously to a quadratic Kerr effect). To observe the photoinduced SH and the photoinduced light scattering, it is necessary to have large values of the optically induced electric-field strengths. According to the coherent photogalvanic effect [Eqs. (1)–(3)], the low value of the conductivity in oxide glasses favors an accumulation of the photoinduced effective electrostatic field (10^4 – 10^6 V/cm) in these materials and such values of the field are sufficient for the occurrence of the observed phenomena.

The above-presented approach gives an adequate description of the optical poling process. However, it is impossible to explain the observed anisotropy of the light absorption kinetics in the region of high induced optical field (effective electric-field strength larger than $\sim 10^4$ V/cm). The dependence of the independently measured integrated absorption indicates an important role played by the optical poling and

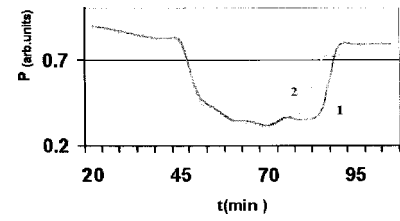


FIG. 7. Theoretically simulated temporary dependence of the photoinduced SH for two light polarizations: 1, \perp ; 2, \parallel .

that the photodarkening may be neglected in this case. For the explanation of the observed phenomenon, it is necessary to take into account the occurrence of the photoinduced anisotropy diffusion processes determined by the effective depopulation kinetics of the appropriate trapping levels. In particular, the polarized dependencies of the time-dependent absorption may indicate a significant role of the photoinduced phonons defining the anisotropy of the decays of photocarriers with respect to the photoinduced light polarization.

The major role in the observed kinetics should be played by long-lived photopolarized states originating from the glass trapping levels and phonons (due to the piezoelectric-electrostricted effects) created by the high photoinduced electric-field strengths, Eq. (3). The mechanical stress second-rank tensor σ_{ij} induces a phonon displacement field with the displacement vectors directed along the i and j directions. Due to light polarization, the ionic displacement (determining the phonons) will be different for the two light polarizations (for parallel and perpendicular directions with respect to the incident light). The considered phonons interact with the localized trapping states, changing substantially their living times and polarizabilities. Particularly, there occur the long-lived polaron (autolocalized phonon) states causing an anisotropy of diffusion coefficients D . So during the photoinducing process, we have two anisotropy coefficients of diffusion: D_{\perp} and D_{\parallel} with respect to the direction of light polarization.

As a consequence, occupation of the trapping levels responsible for the electrostatically macropolarized states should decrease:

$$N(t) = N_0 \exp(-x^2/D_{\perp, \parallel} t), \quad (4)$$

where N_0 is the effective number of trapping levels before phototreatment, x is the effective distance of the photocarriers with respect to the photoinduced border at time t .

During the illumination by the polarized light, the diffusion coefficient D of the bound electron-phonon carriers decreases [15], favoring the additional polarization of the excited trapping levels. The appearance of additional number of trapping levels leads to the occurrence of larger number of delocalized states within the forbidden energy gap (see Fig. 7). As a consequence, the absorption coefficient for the steady-state levels participating in the nonlinear cascading processes should stimulate a large absorption of the SH, which was observed in our experiments.

For the simulations of photoinduced electron-phonon processes (effectively changing the diffusion coefficients D), we performed microscopic calculations using the Green func-

tion. The general formalism is similar to the earlier described in Refs. [19,20]. The electron-phonon potential was calculated within a nonlinear electron-phonon anharmonic approach. We have done the calculations for the mixed electron-phonon basis set.

The carrier's occupation dynamics caused by photoinduced changes was calculated using the description of the carrier kinetics presented in the Ref. [20]. To include the optically induced lattice deformations within the Green function, we took into account deformation localization, allowing us to use the Dyson relations [19]. Using the Green-function formalism for the photoinduced electron-phonon anharmonic states and an approach developed for the carrier kinetics [19,20], we have simulated the absorption of light for the two light polarizations (see Fig. 7).

From Fig. 7 one can see an occurrence of anisotropy in the kinetics of SH absorption after 70 min of optical treatment. Comparison with the experimental data (see Fig. 3) allows us to conclude that the photoinduced phonons effectively interact with the glass trapping levels stimulating the observed anisotropy of the SH absorption kinetics.

IV. CONCLUSIONS

A large increase (up to $\geq 10^3$ times) of the absorption of second-harmonic radiation by optical poling of oxide glass was discovered. We have observed anisotropic kinetics of the observed effect after the optical poling interruption. It was found that the observed absorption is caused by the restriction of the poling process. The performed microscopic simulation showed that the observed effect is the result of a competition between the charge separation by the local trapping levels due to electrostricted photoinduced phonons and the recombination diffusion of the photocarriers. The performed quantum chemical evaluations have shown that other nonlinear optical phenomena (such as intensity-dependent refractive index and fourth-harmonic generation) give a relatively small contribution to the observed SH's absorption. Due to the occurrence of additional number of bound electron-phonon states (polarons), we have observed additional absorption for the doubled frequency that is unambiguously confirmed experimentally and by appropriate quantum chemical theoretical simulations.

-
- [1] B. Ya. Zel'dovich, Yu. E. Kapitsky, and V. M. Churikov, *JETP Lett.* **53**, 77 (1991).
 - [2] M. K. Balakirev, M. V. Entin, V. A. Smirnov, and L. I. Vostrikova, *JETP Lett.* **63**, 176 (1996).
 - [3] B. P. Antonyuk, *Opt. Commun.* **181**, 151 (2000).
 - [4] M. K. Balakirev and V. A. Smirnov, *JETP Lett.* **61**, 544 (1995).
 - [5] E. M. Dianov, P. G. Kazansky, and D. Yu. Stepanov, *Sov. J. Quantum Electron.* **17**, 926 (1990).
 - [6] U. Osterberg and W. Margulis, *Opt. Lett.* **11**, 516 (1986).
 - [7] T. J. Driscoll and N. M. Lawandy, *J. Opt. Soc. Am. B* **11**, 355 (1994).
 - [8] E. M. Dianov and D. S. Starodubov, *Sov. J. Quantum Electron.* **22**, 419 (1995).
 - [9] F. Charra, F. Kajzar, J. M. Nunzi, F. Raimond, and E. Idiart, *Opt. Lett.* **18**, 941 (1993).
 - [10] J. Wasylak, J. Kucharski, I. V. Kityk, and B. Sahraoui, *J. Appl. Phys.* **85**, 425 (1999).
 - [11] Y. Quiquempois, A. Villeneuve, D. Dam, K. Turcotte, J. Muller, G. Stegeman, and S. Lacroix, *Electron. Lett.* **36**, 733 (2000).
 - [12] E. Lopez-Lago, V. Couderc, L. Griscom, F. Smektala, and A. Barthelemy, *Proceedings of CLEO/Europe-IQEC 2000*, Nice, France, 2000 (unpublished).
 - [13] B. P. Antonyuk and V. B. Antonyuk, *Sov. J. Adv. Phys. Sci.* **171**, 61 (2001).
 - [14] M. K. Balakirev, V. A. Smirnov, and L. I. Vostrikova, *Opt. Commun.* **178**, 181 (2000).
 - [15] E. M. Baskin and M. V. Entin, *JETP Lett.* **48**, 601 (1988).
 - [16] V. O. Sokolov and V. B. Sulimov, *Phys. Status Solidi B* **187**, 189 (1995).
 - [17] *Clear Optical Glass. Physical-Chemical Characteristics. Basic Parameters* (Standard, Moscow, 1999); *Catalogue of the Optical Glasses* (Galeas, Kharkov, 1999); *Parameters of Optical Glasses* (Moscow, 1999), p. 556.
 - [18] M. C. Farries and M. E. Fermann, *Electron. Lett.* **24**, 294 (1989).
 - [19] L. A. Tiagnyriadko, I. V. Kityk, and I. N. Yashchishin, *Phys. Chem. Glasses* **20**, 404 (1994).
 - [20] I. V. Kityk and B. Sahraoui, *Phys. Rev. B* **60**, 942 (1999).